David M. Lawrence
ENVS 691 Laboratory Exercise No. 4

IRRADIANCE AND PRODUCTION

The effects of irradiance on productivity were evaluated using a model of a river/estuary system. The basin, discharge and tide characteristics of the modeled river/estuary system were derived from those employed in an earlier exercise. To that system were added turbidity, light attenuation with depth, and irradiance parameters to determine the amount of energy available to drive gross primary productivity. Irradiance was obtained from a solar radiation model I developed that uses date, latitude, and other site parameters to estimate direct and diffuse incoming solar radiation (insolation) for the 15th day of each month was obtained from a solar radiation model I developed to estimate, among other things, direct and diffuse solar radiation incident upon a surface. Radiation model output (W m^{-2}) was converted to total photosynthetically active radiation (PAR; µmol photos m^{-2} s^{-1}) in a two-step process. First, the proportion of PAR in visible light (both direct and diffuse) was assumed to be 46% – within the range of reported values. Second, the direct PAR fraction was multiplied by 4.57, while the diffuse PAR fraction was multiplied by 4.24 (Britton & Dodd, 1976; Dye, 2004). Solar radiation model results and conversions are presented in Table 1.

River depth is variable, but the estuarine segment gradually gets shallower as one moves from the head of the estuary to its mouth (Figure 1). Turbidity generally decreases as one moves from upstream to downstream in the riverine segments, but increases again at the head of the estuary where there is greatest mixing of riverine and marine waters and decreases again toward the mouth of the estuary (Figure 2). In all segments, turbidity increases with flow.

Conversely, mean irradiance of the waters decreases during periods of greater discharge – though toward the mouth of the estuary, irradiance during medium- and low-flow periods

converge as the shallower depths allows light to reach the bottom (Figure 3a and Figure 3b). This trend holds for all seasons. The differences in irradiance among the flow regimes decrease in winter months and increase in the summer.

Respiration is typically greater than gross primary production (GPP) in the riverine segments (Figures 4a through Figure 4f). In most cases, GPP exceeds respiration only in the lower segments of the estuary, though the model predicts that respiration will seasonally exceed gross primary productivity in all systems segments (see December data in Figure 4f). The variability in productivity likely as a lot to do with penetration of light through the water column. Where water is shallower, or where solar angles are higher and daylength longer, a greater proportion of autotrophic or potentially autotrophic organisms throughout the water column receive the energy they need to drive photosynthesis (Bukaveckas, Barry, Beckwith, David, & Lederer, 2011).

REFERENCES

Britton, C. M., & Dodd, J. D. (1976). Relationships of photosynthetically active radiation and shortwave irradiance. *Agricultural Meteorology*, *17*(1), 1-7.

Bukaveckas, P., Barry, L., Beckwith, M., David, V., & Lederer, B. (2011). Factors Determining the Location of the Chlorophyll Maximum and the Fate of Algal Production within the Tidal Freshwater James River. *Estuaries and Coasts*, *34*(3), 569-582. doi: 10.1007/s12237-010-9372-4

Dye, D. G. (2004). Spectral composition and quanta-to-energy ratio of diffuse photosynthetically active radiation under diverse cloud conditions. *J. Geophys. Res.*, *109*(D10), D10203. doi: 10.1029/2003jd004251

Table 1. Monthly modeled values of solar position (declination, radius vector), incoming solar radiation (insolation), and photosynthetically active radiation (PAR) for Eastport, Maine (latitude 44.9 °N).

	Solar Variables		Insolation (W m^{-2})			PAR (µmol photons m^{-2} s^{-1})		
Month	Declination	Radius Vector	Top of Atmosphere	Direct Surface	Diffuse Surface	Direct PAR	Diffuse PAR	Total PAR
Jan	21.2 °S	0.969	141.08	106.71	10.83	224.33	21.12	245.40
Feb	13.2 °S	0.977	207.16	164.81	11.85	346.46	23.11	369.52
Mar	2.7 °S	0.990	289.95	241.00	11.42	506.63	22.27	528.85
Apr	9.5 °N	1.007	379.46	325.69	9.81	684.67	19.13	703.75
May	18.8 °N	1.023	441.34	384.07	8.77	807.39	17.11	824.46
Jun	23.3 °N	1.032	466.78	406.76	9.00	855.09	17.55	872.60
Jul	21.5 °N	1.033	451.55	394.25	8.32	828.79	16.23	844.98
Aug	13.7 °N	1.024	401.35	345.94	9.64	727.24	18.80	745.99
Sep	2.1 °N	1.008	319.29	269.88	10.33	567.34	20.15	587.44
Oct	9.7 °S	0.992	229.13	186.83	10.84	392.75	21.14	413.85
Nov	19.2 °S	0.977	156.01	118.86	11.55	249.87	22.53	272.34
Dec	23.3 °S	0.969	125.42	91.91	11.11	193.21	21.67	214.83

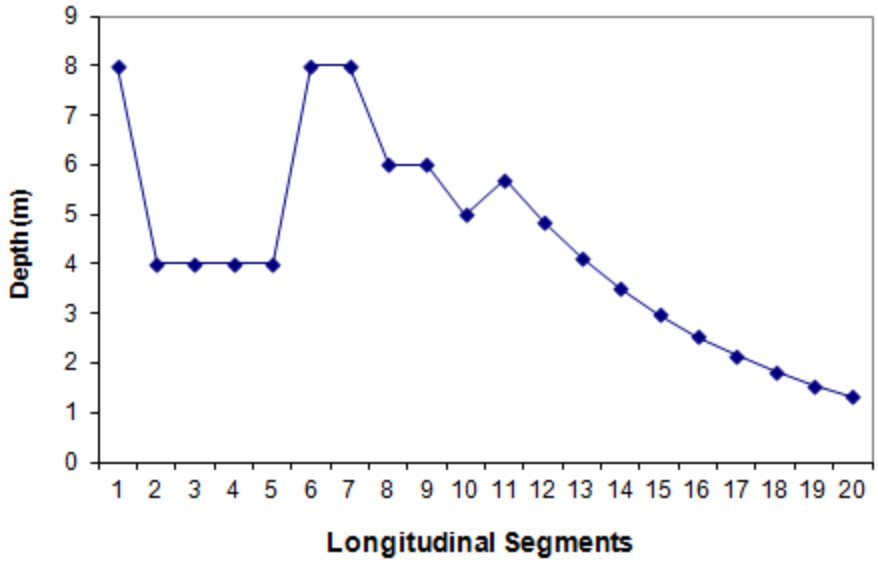

Figure 1. Plot of depth (m) versus segment of the modeled river/estuary system. The first 10 segments represent the riverine portion, the last 10 the estuary. Each segment is 20 km long.

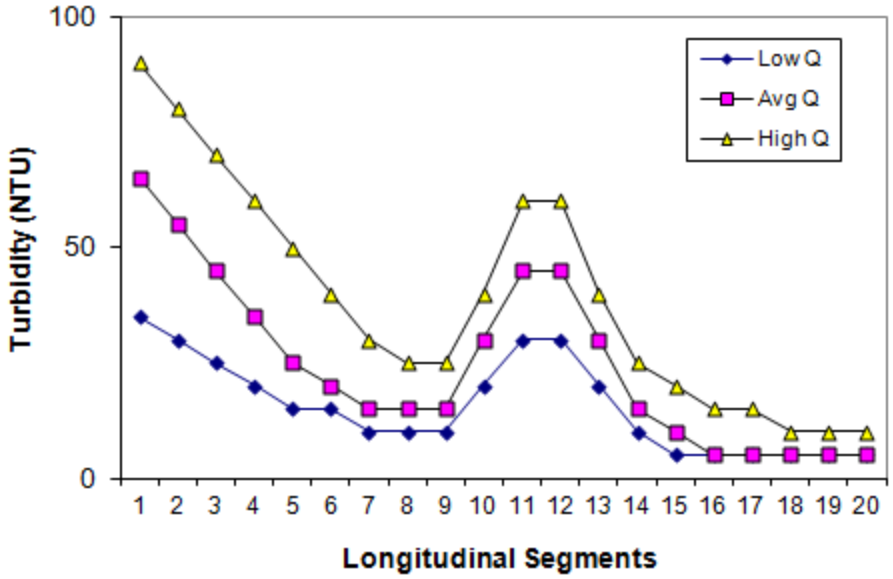

Figure 2. Plot of turbidity (NTU) versus segment of the modeled river/estuary system.

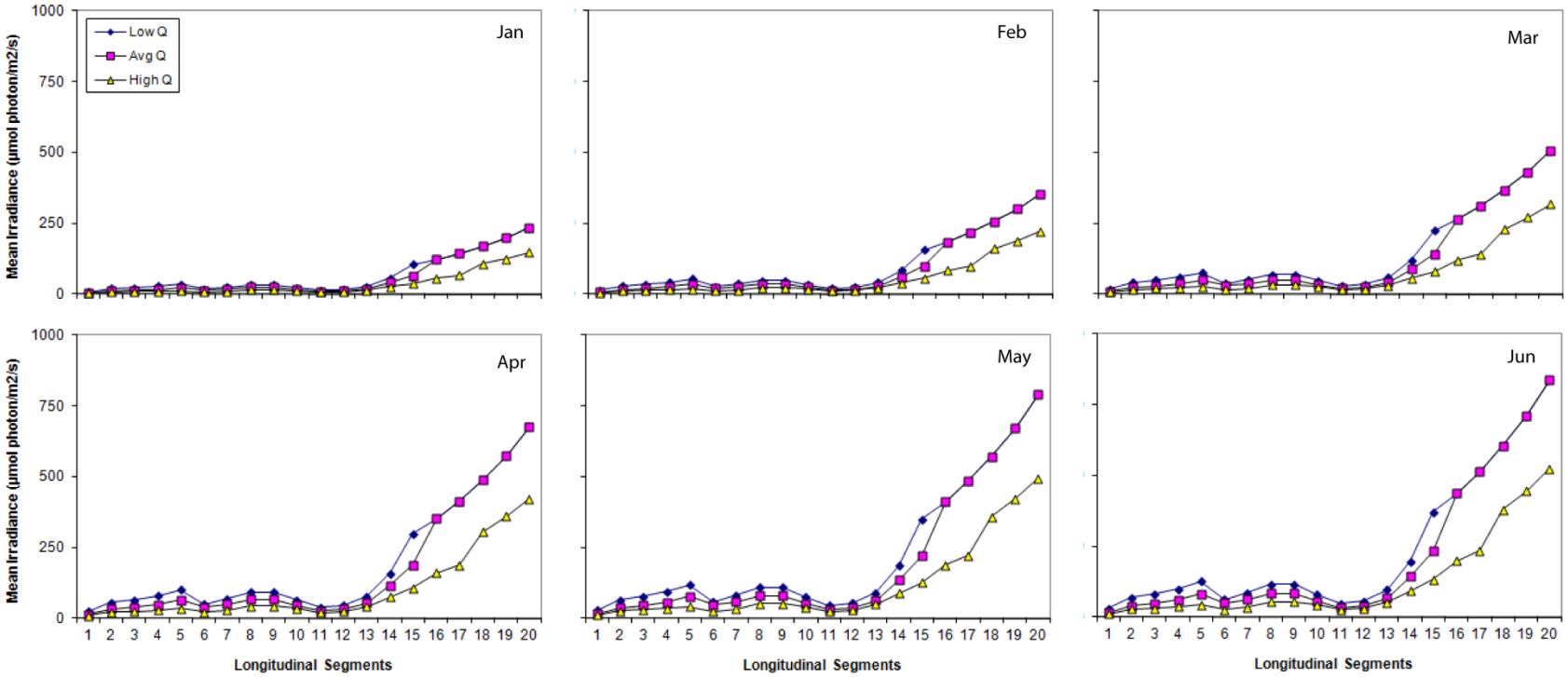

Figure 3a. Mean irradiance (µmol photons m^{-2} s^{-1}) versus segment for the modeled river/estuary system under each of three flow (Q; m s^{-1}) regimes (high, medium, and low) for the months January through June.

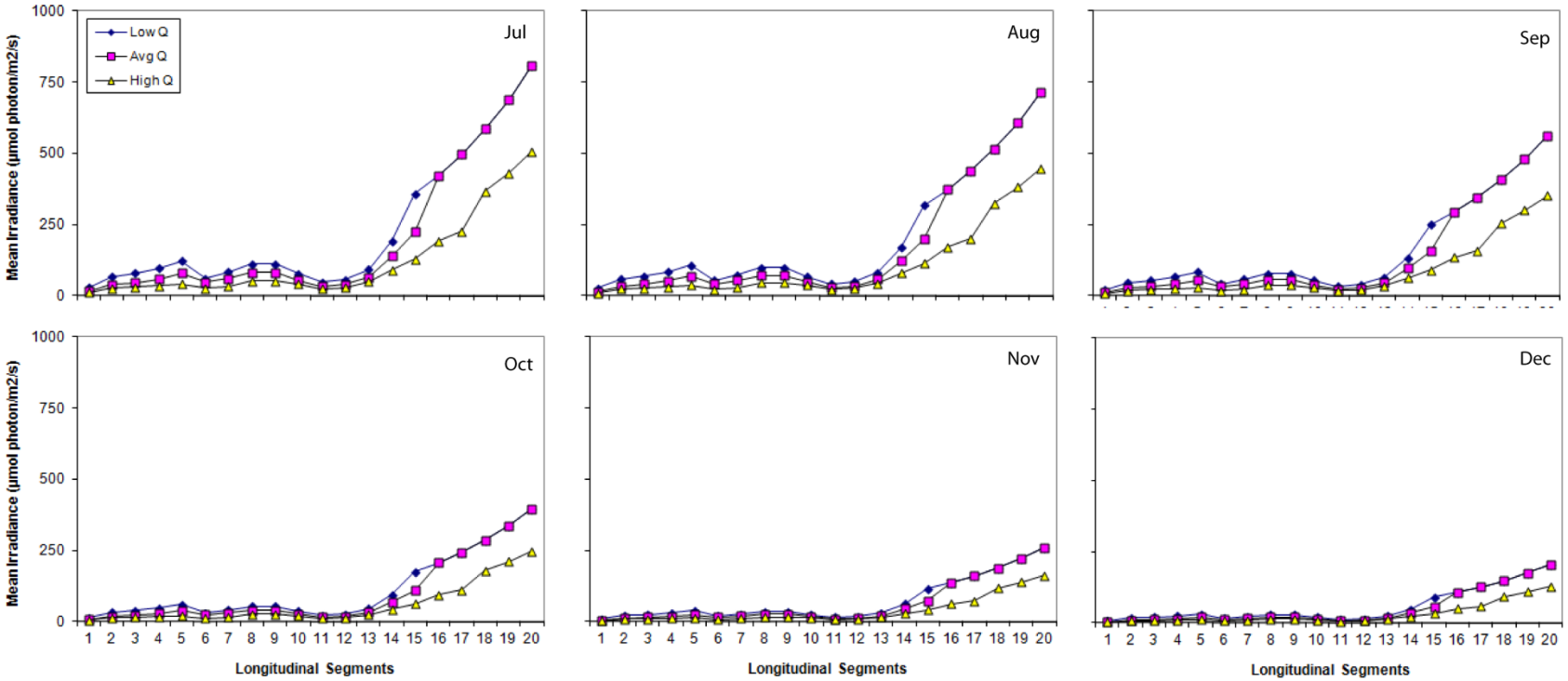

Figure 3b. Mean irradiance (µmol photons m^{-2} s^{-1}) versus segment for the modeled river/estuary system under each of three flow (Q; m s^{-1}) regimes (high, medium, and low) for the months July through December.

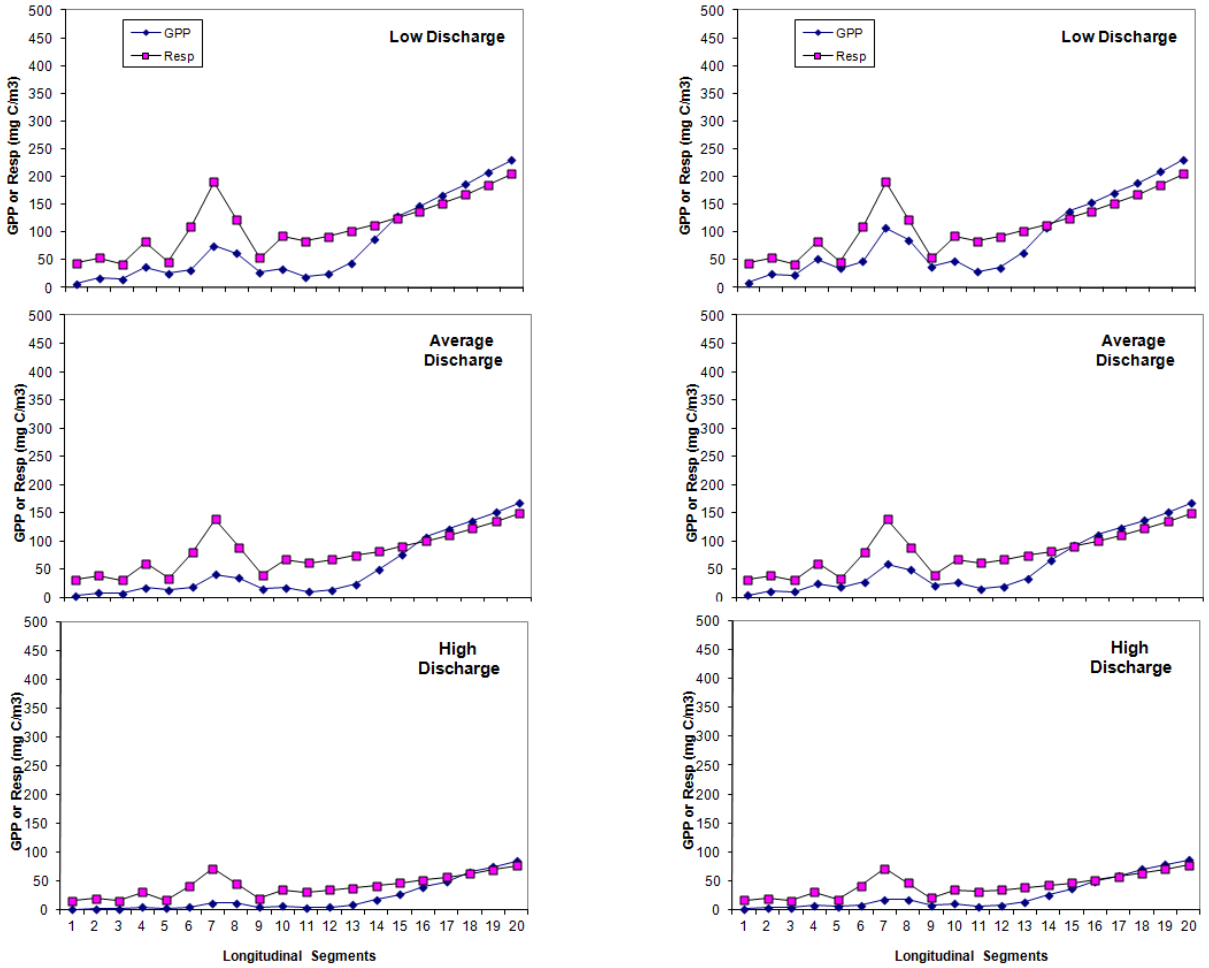

Figure 4a. Plot of gross primary productivity (GPP; mg C m^3) and respiration (Resp; mg C m^3) versus segment of the modeled river/estuary system under each of three discharge regimes (high, medium, and low) for the month of January (left) and February.

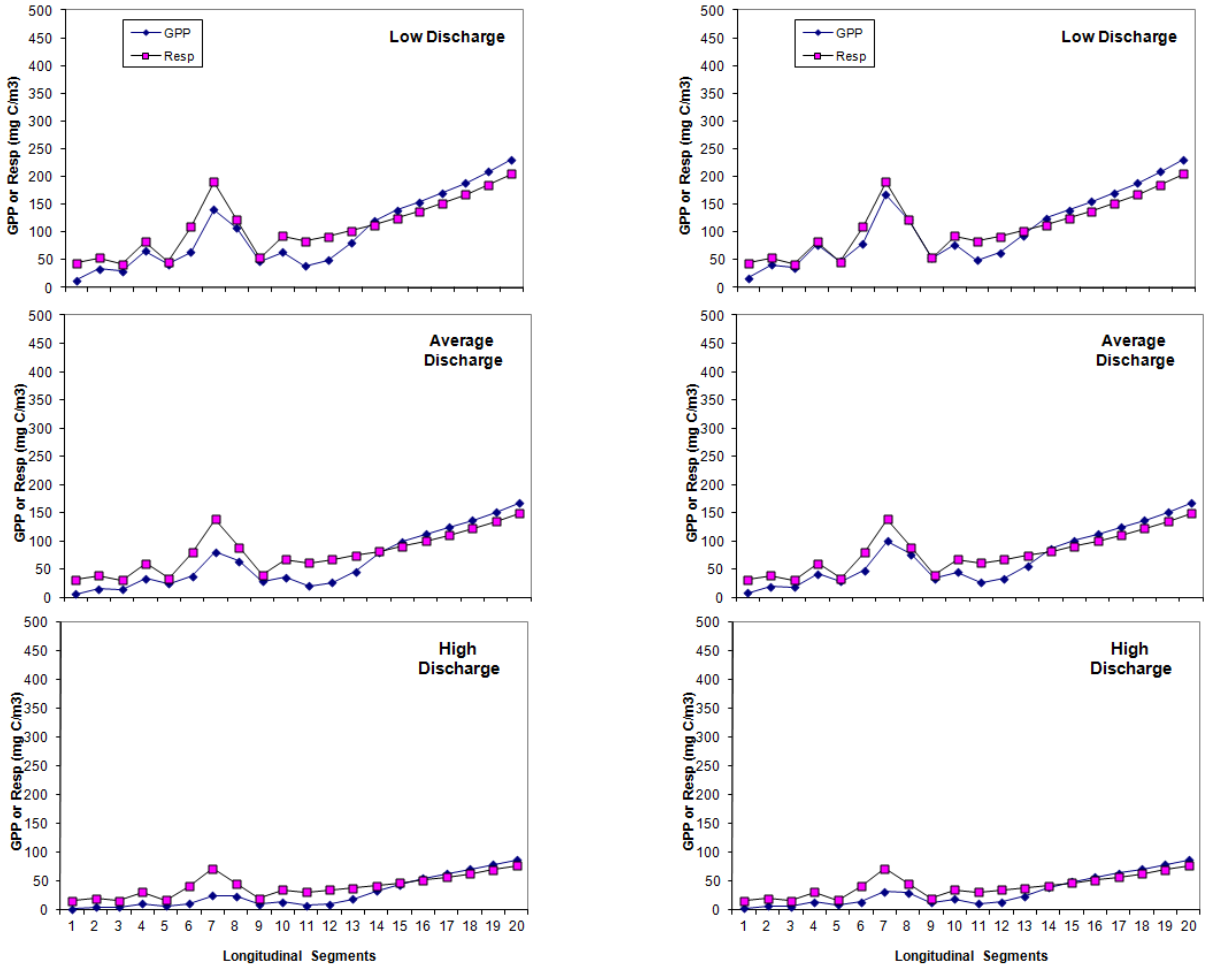

Figure 4b. Plot of gross primary productivity (GPP; mg C m^3) and respiration (Resp; mg C m^3) versus segment of the modeled river/estuary system under each of three discharge regimes (high, medium, and low) for the month of March (left) and April.

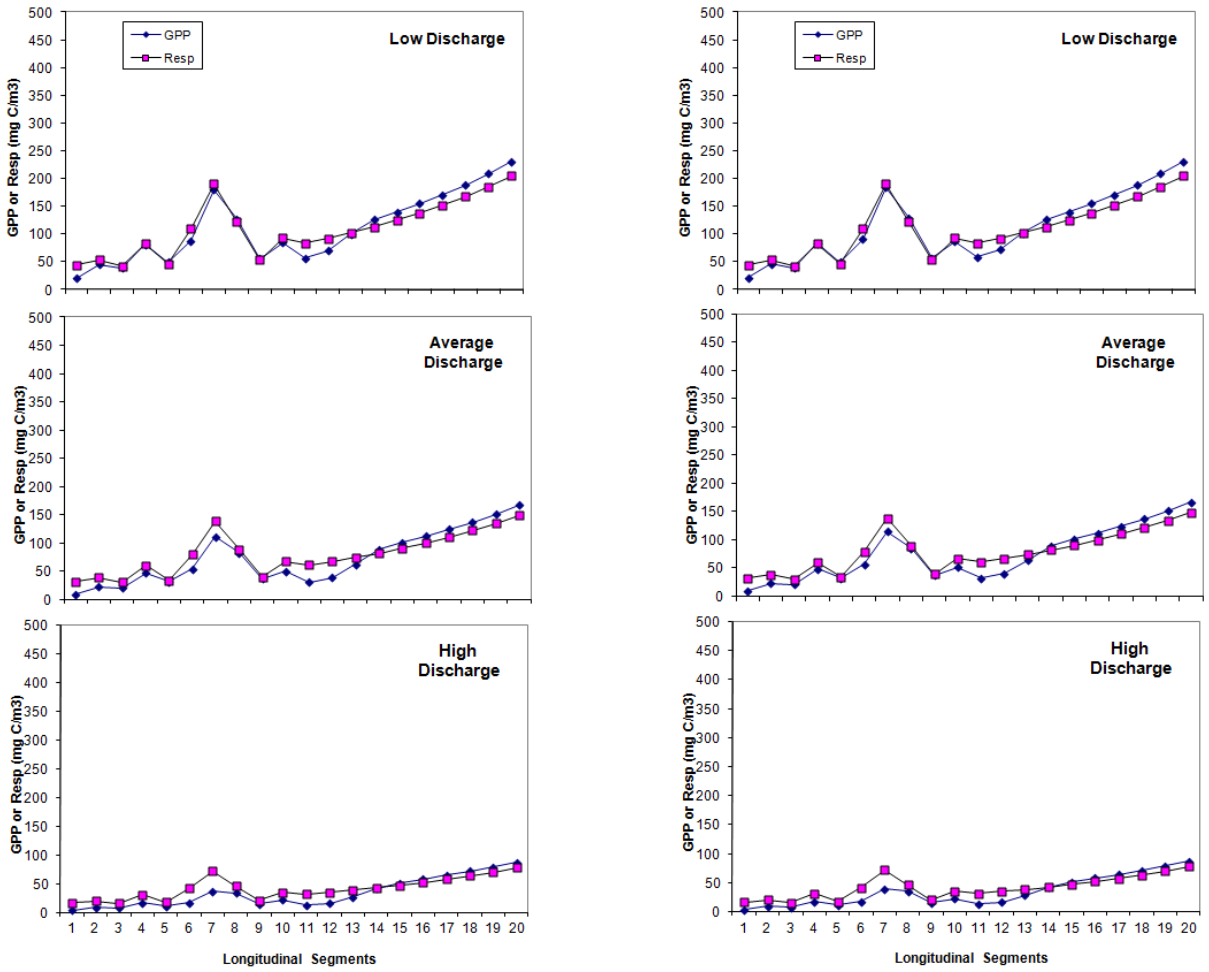

Figure 4c. Plot of gross primary productivity (GPP; mg C m^3) and respiration (Resp; mg C m^3) versus segment of the modeled river/estuary system under each of three discharge regimes (high, medium, and low) for the month of May (left) and June.

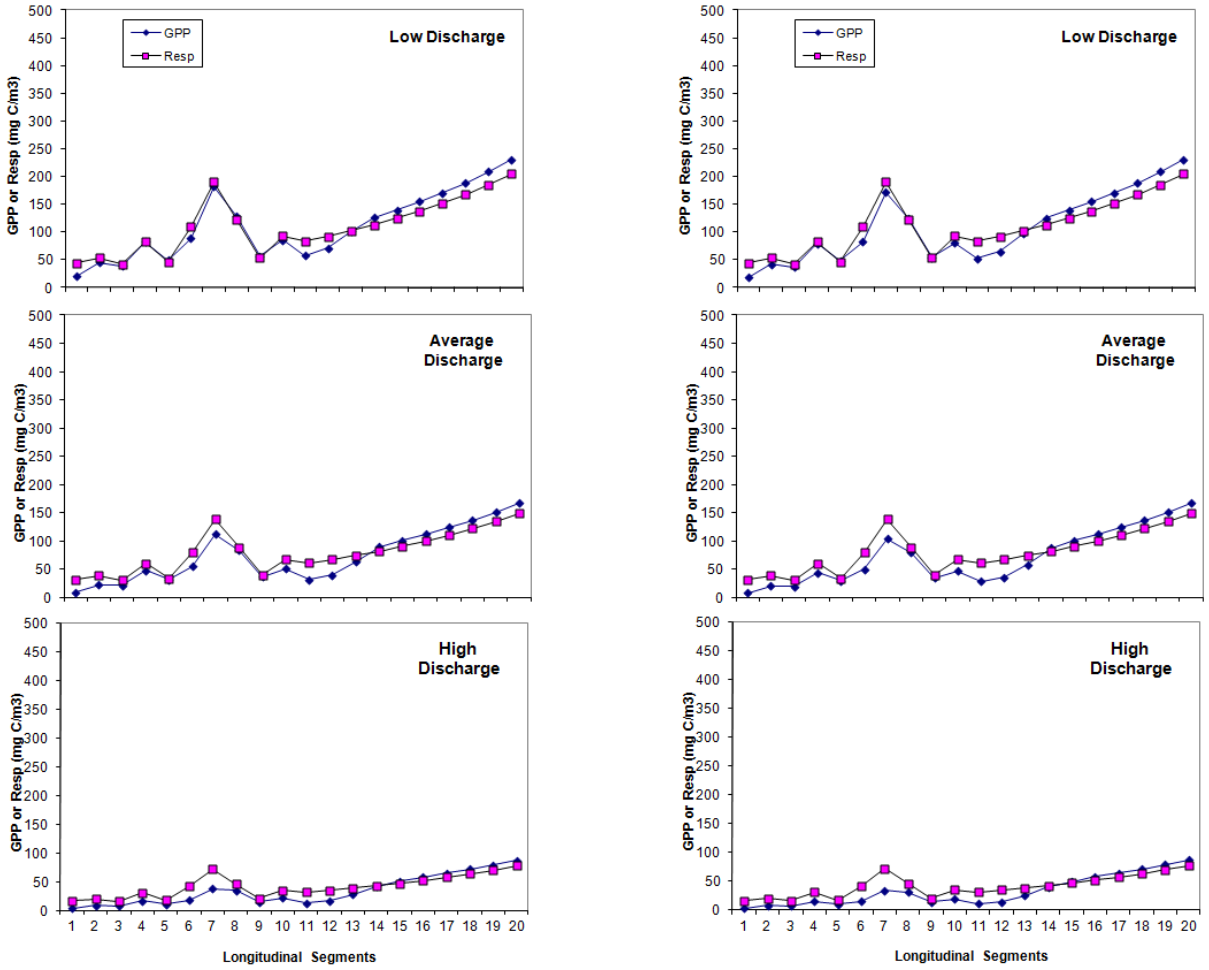

Figure 4d. Plot of gross primary productivity (GPP; mg C m^3) and respiration (Resp; mg C m^3) versus segment of the modeled river/estuary system under each of three discharge regimes (high, medium, and low) for the month of July (left) and August.

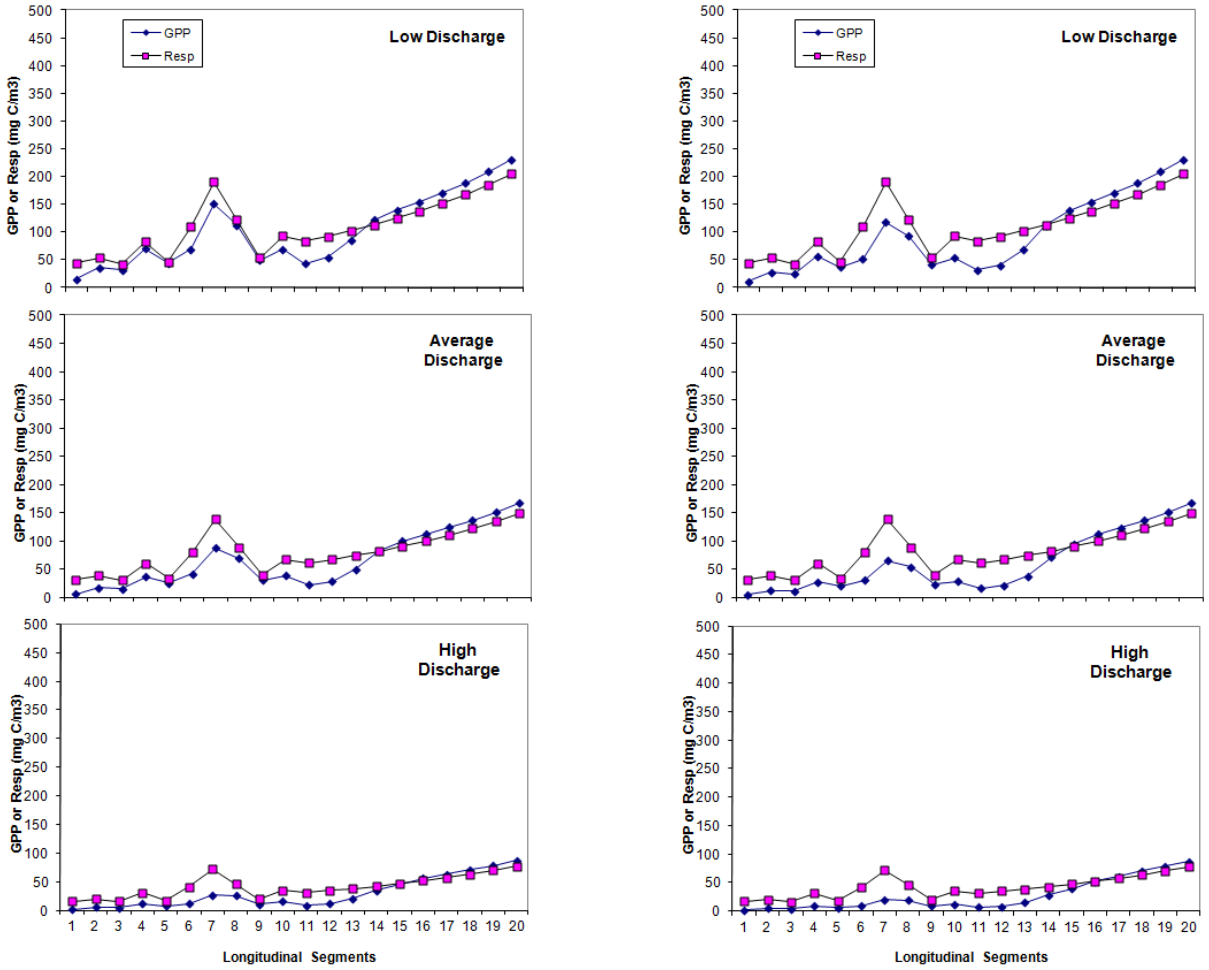

Figure 4e. Plot of gross primary productivity (GPP; mg C m^3) and respiration (Resp; mg C m^3) versus segment of the modeled river/estuary system under each of three discharge regimes (high, medium, and low) for the month of September (left) and October.

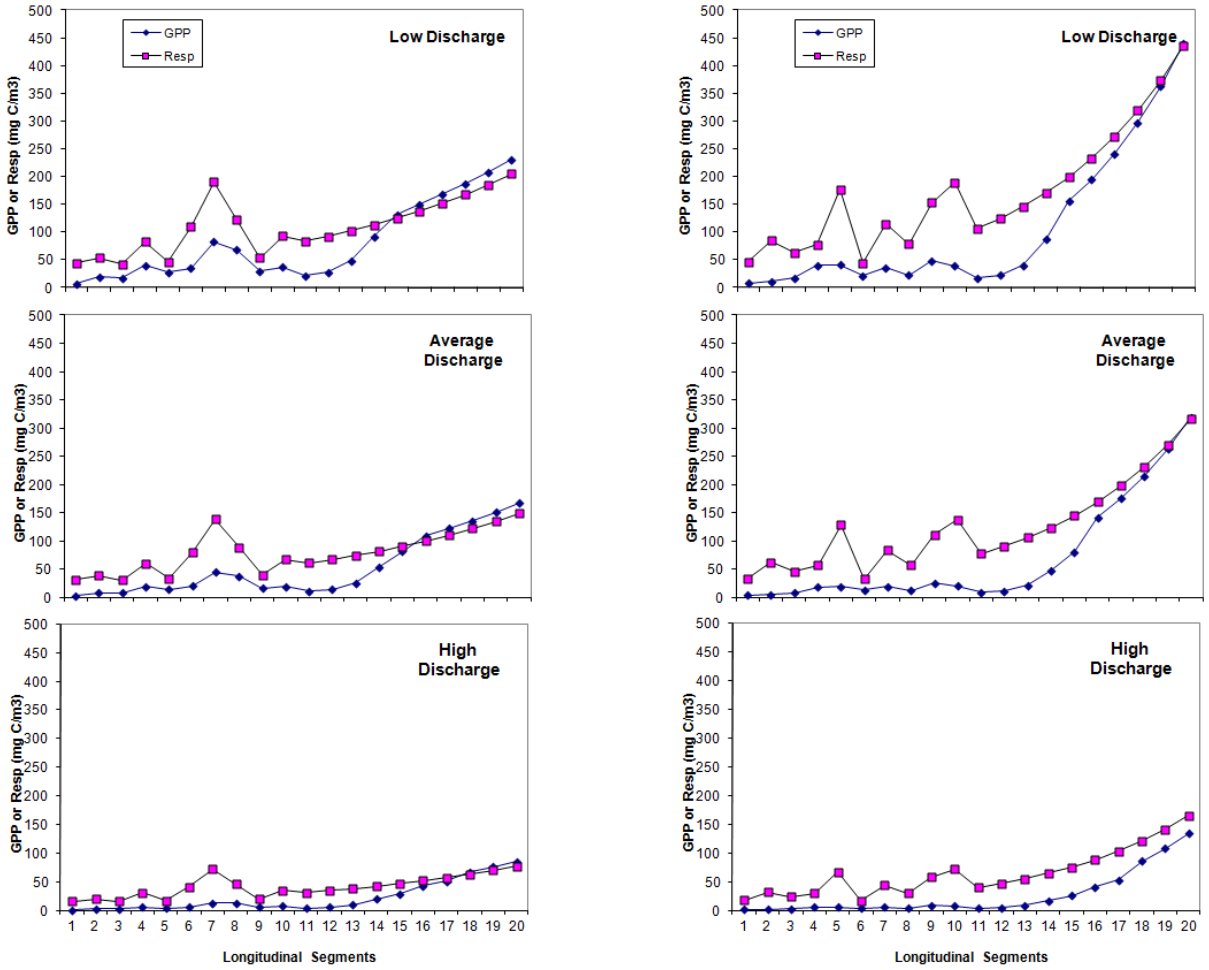

Figure 4f. Plot of gross primary productivity (GPP; mg C m^3) and respiration (Resp; mg C m^3) versus segment of the modeled river/estuary system under each of three discharge regimes (high, medium, and low) for the month of November (left) and December.